A small subset of artemisinin induced dormant *P. falciparum* parasites maintain mitochondrial membrane potential and resume growth *in vitro*.

Christopher L. Peatey[1,2#], Marina Chavchich[1], Nanhua Chen[1], Karryn J. Gresty[1,2], Karen-Ann Gray[1,2], Michelle L Gatton[3], Norman C. Waters[4] and Qin Cheng[1,2]

[1]Drug Resistance and Diagnostics, Australian Army Malaria Institute, Brisbane, 4051 Australia; [2]Clinical Tropical Medicine, QIMR Berghofer Medical Research Institute Brisbane 4006 Australia; [3]School of Public Health and Social Work, Queensland University of Technology, Brisbane 4001, Australia; [4]Walter Reed Army Institute of Research, Malaria Vaccine Branch, Military Malaria Research Program, Silver Spring, 20901 MD, USA.

#corresponding author.

Key words: *P. falciparum*, artemisinin, dihydroartemisinin (DHA), dormancy, mitochondrial membrane potential

Foot note:

None of the authors have any commercial or other associations that may pose a conflict of interest regarding this research. This work was supported by the National Health and Medical Research Council of Australia [grant number:

1021273]. This work has not been previously presented at any scientific meetings.

The corresponding author is:

Dr Christopher L. Peatey

Australian Army Malaria Institute

Gallipoli Barracks, Enoggera

Queensland, Australia. 4053

Tel: 61-7-3332-4837

Fax: 61-7-3332-4800

christopher.peatey@defence.gov.au

Abstract

Artemisinin induced dormancy is a proposed mechanism for failures of mono-therapy and is linked with artemisinin resistance in *Plasmodium falciparum*. The biological characterization and dynamics of dormant parasites are not well understood. Here we report that following dihydroartemisinin (DHA) treatment *in vitro*, a small subset of morphologically dormant parasites was stained with rhodamine 123 (RH), a mitochondrial membrane potential (MMP) marker, and persisted to recovery. FACS sorted RH-positive parasites resumed growth at 10,000/well while RH-negative parasites failed to recover at 5 million/well. Furthermore, transcriptional activity for mitochondrial enzymes was only detected in RH-positive dormant parasites. Importantly, after treating dormant parasites with different concentrations of atovaquone, a mitochondrial inhibitor, the recovery of dormant parasites was delayed or stopped. This demonstrates that mitochondrial activity is critical for survival and regrowth of dormant parasites and that RH staining provides a means of identifying these parasites. These findings provide novel paths for studying and eradicating this dormant stage.

Introduction

Artemisinin-based combination therapies are the frontline treatment for uncomplicated *P falciparum* malaria and their use has contributed to the worldwide reduction of malaria incidence rates [1, 2]. Prior to recent reports of emerging resistance to artemisinins [3-6] evidence showed up to 50% of patients suffered treatment failures after artemisinin monotherapy, despite parasites being sensitive to artemisinin class compounds [7]. Antimalarial combinations have significantly reduced the rate of recrudescence. Understanding mechanisms underlying frequent recrudescence following artemisinin monotherapy and increasing efficacy of combination therapies will greatly improve future treatments.

Recently, treatment failure has been attributed to artemisinin sensitive ring stage parasites entering growth arrest, referred to as dormancy [8, 9], following artemisinin monotherapy and resuming growth several days later. Artemisinin induced dormancy has been observed *in vitro* [9-11], as well as *in vivo* in a mouse malaria model [12]. Proposed to be a stress-response that helps parasites survive artemisinin pressure [13], dormancy is linked to the ability of parasites to recover from artemisinin treatment at concentrations up to 7000 times the initial IC_{50} for up to 96 hours [11]. Teuscher *et al.*, [14] demonstrated that decreases in the number of parasites entering the dormant phase may be an indicator of the parasite line's acquiring resistance to artemisinin. Similar findings were reported in another laboratory generated artemisinin resistant line [11] and also in artemisinin resistant field isolates, as increasing ring survival rates [15]. These studies indicate that dormancy is linked with an artemisinin

resistance phenotype and understanding how parasites initiate and maintain the dormant state is important to combat artemisinin resistance.

Although the phenomenon of dormancy is accepted there are conflicting views about the morphology of dormant parasites. Teuscher *et al.* [9] and Tucker *et al.* [10] described dormant parasites, whilst similar to the collapsed nuclei of pyknotic forms, retaining some blue cytoplasm and condensed red chromatin. This morphology is different from typical ring stage parasites. Witkowski *et al.* [16] reported that after treatment with 700 nM dihydroartemisinin (DHA) the morphologically normal looking ring stage parasites underwent cell cycle arrest and maintained ring morphology for up to 48 hours. Establishing a biomarker will help identify dormant parasites and assist investigations into the mechanism of dormancy.

The dormancy phenomenon is not uncommon in microorganisms. *S. cerevisiae* enters a dormant phase during periods of unfavourable growth conditions, where cells stop glycolysis and start metabolising ethanol through the TCA cycle [17]. Recent studies show that mutant yeast species, deficient in genes encoding proteins used for oxidative phosphorylation and other mitochondrial functions, fail to survive the dormant phase [18]. This indicates that mitochondria are vital to the maintenance of yeast cells when they enter dormant phase.

The mitochondria of malaria parasites differs from other eukaryotic cells. It is present in all stages including ring stage and shares a close association with the apicoplast [19]. The proximity of these organelles has been hypothesised as necessary for metabolic interaction [19, 20]. The malarial mitochondrion is involved in metabolic

pathways including pyrimidine biosynthesis, iron-sulfur cluster and heme biogenesis, the biosynthesis of ubiquinone and tricarboxylic acid metabolism [21]. Chen *et al.* [22] recently reported that both the apicoplast and mitochondrion, remain active in dormant rings, suggesting an important role for these organelles in the survival and recovery of dormant parasites.

To confirm dormant parasites maintain some mitochondrial function and if this could be used as a biomarker, a mitochondrial dye, Rhodamine 123 (RH), was used for detection, characterization of the morphology and dynamics of dormant parasites. RH binds to the mitochondrial membrane of cells and is an indicator of MMP, essential for mitochondrial function and thus cell viability. Mitochondrial activity has been measured in another apicomplexan, *Toxoplasma gondii* using RH [23]. RH has been used to identify live *P.falciparum* parasites by flow cytometry [24-27] and show that parasites treated with antimalarial drugs lost RH staining and never resumed growth [25].

Here we report that following DHA treatment *in vitro*, a small subset of morphologically dormant parasites was stained with RH and only RH-stained parasites resumed growth. Furthermore, transcriptional activity of mitochondrial enzymes was only detected in RH+ve dormant parasites. Importantly, after treating dormant parasites with atovaquone, a mitochondrial inhibitor, we successfully delayed the recovery of dormant parasites. This demonstrates that mitochondrial activity is critical for survival and regrowth of dormant parasites. RH staining can be used as a means of distinguishing dormant from dead parasites in DHA treated cultures. These findings provide novel methods for studying and eradicating dormant parasites.

Methods

Parasite Cultivation

P.falciparum strain W2 (Indochina), was cultivated using standard techniques in RPMI 1640 HEPES (Sigma Aldrich) culture medium supplemented with 10% human plasma and at 3% haematocrit [28]. Prior to each experiment, parasites were synchronized at ring stage using two rounds of 5% D-sorbitol treatment [29].

Induction and selection of dormant parasites

Synchronised ring stage parasites were treated with 200 ng/ml DHA (Sigma Aldrich) for 6 hours then washed with culture medium. The treated culture was passed through a magnetic column (25 MACS CS separation columns; Miltenyi Biotec) on days 1 to 3 as previously described [9]. Parasite samples were collected before and daily after DHA treatment in investigations detailed below. Where experiments used Day 2 post-treatment parasites approximately 50% of parasites were morphologically dormant and remaining parasites were dead [22]. Ring stage W2 parasites were treated with atovaquone (ATQ) (61 µM, for 24 hours) - a known inhibitor of cytochrome b-c_1 complex – that results in a loss MMP.

Investigating dynamics of RH and SYBR Green (SG) stained parasites following DHA treatment

Following DHA, or atovaquone treatment, a daily sample (100 µl) was stained with either RH (Sigma Aldrich) at 10 µg/ml or SG (10,000x concentration, (Sigma Aldrich) diluted to 20x concentration, as described in [26] [30] for flow cytometry analysis. Thin blood smears were Giemsa stained and examined by microscopy.

For FACS analysis, parasites were washed three times in 1xPBS and then analysed in a FACS Canto II (Becton Dickson, San Jose, CA) using the 488nM blue laser to determine RH or SG stained fraction. Flow cytometry data, collected from 100,000 events, were analysed using FlowJo software (Treestar). Stained uninfected RBC (controls) were gated out and referred to as RH-ve or SG-ve fractions and subtracted from treatment samples. All other fluorescence events were considered RH+ve or SG+ve events. The experiment was repeated 3 times using different cultures.

Investigating recovery of RH and SG stained and unstained parasites

On Day 2 post DHA treatment, parasites were stained with RH, resuspended in 1xPBS and sorted using a FACS Aria live cell sorter (Becton Dickson, San Jose, CA). Both RH+ve and RH-ve fractions were collected. The RH-ve fractions, were subsequently stained with SG and resorted (RH-ve/SG+ve). Both RH+ve and RH-ve/SG+ve parasites were then plated out in 96-well plates in triplicate, containing 10,000, 1,000, 100 and 10 sorted parasites/well. A culture containing RH-ve/SG+ve parasites at 5,000,000 parasites/well was also included. Plates were washed in PBS and returned to culture conditions. Parasites were monitored every 96 hours, by microscopy and counted with RH and SG, using a FACS Canto II on the high throughput sampler option (HTS), to detect parasite growth for 25 days or until they reached 10% parasitemia. The experiment was repeated 3 times.

Investigating micrographs of dormant parasites

An aliquot of RH+ve and RH-ve/SG+ve parasites sorted on Day 2 post DHA treatment was Geimsa stained and examined by light microscope. Parasite images

were captured with a Jenoptik Progress C14 camera system (Jenoptik, Jena, Germany) operating Image-Pro software.

Investigating mitochondrial and apicoplast gene transcription

20,000 RH+ve untreated ring stage parasites and 20,000 each of RH+ve, RH-ve/SG+ve DHA treated ring stage parasites (Day 2 post treatment) were used to measure transcription of mitochondrial enzymes. RNA isolation and cDNA synthesis were performed as previously described [22]. Transcriptions of three genes encoding mitochondrial enzymes including cytochrome c oxidase subunit II (*coxii*), flavoprotein subunit of succinate dehydrogenase (*sdha*) and ubiquinnol-cytochrome c reductase iron-sulfur subunit (*uqcr*), and two genes encoding apicoplast enzymes, lipoyl synthase (*lipA*) and biotin carboxylase subunit of acetyl CoA carboxylase (*bc*) were examined by real time quantitative PCR using gene specific primers and results normalised as described in [22]. Triplicate samples from three sorts (n=3x3=9) were analysed and the average quantification cycle (Cq value) calculated. These values were compared to those of 20,000 untreated RH+ve parasites to provide a relative proportion for 20,000 DHA treated RH+ve and RH-ve/SG+ve parasites.

Investigating dynamics of RH and SG stained parasites following exposure to other artemisinin derivatives

Parasites were treated with artelenic acid (ARTA) (200 ng/ml) or artesunate (AS) (200 ng/ml) for 6 hrs and monitored daily by FACS using both RH and SG staining as above.

Investigating effects of a mitochondrial inhibitor on DHA-induced dormancy

W2 parasites were treated with DHA (200ng/ml) for 6 hours and subsequently, 24 hrs after initiation of treatment, were exposed to three concentrations of ATQ, 3nM (IC_{90}), 30 nM (10x IC_{90}) and 300 nM (100x IC_{90}) for 24 hrs. Parasite recovery was monitored using RH staining analysed by FACS, against parasites treated with DHA alone.

Results

Dynamics of RH+ve and SG+ve parasites post DHA treatment

Prior to DHA treatment the number of RH and SG stained parasites, were 2.87% ± 0.09 (mean and SD) and 3.06% ± 0.03, respectively. RH+ve parasites averaged 94% SG stained parasites, indicating the majority of parasites have MMP.

After exposure to DHA the number of SG+ve parasites remained unchanged (3.06% ± 0.03) during the first 24 hours, followed by a slight decline to 2.29% ± 0.07 (74.84% of pre-treatment) 48 hours after treatment (Figure 1a). SG+ve parasite counts decreased to 1.03% ± 0.05 (33.66% of pre-treatment) at 72 hours and further dropped to an average of 0.04% (1.57% of pre-treatment) at Day 4 until Day 12. SG+ve parasite counts increased after Day 12, reaching 10% at Day 17 ± 0.3 (mean and SD) (Figure 1a).

In contrast, RH+ve parasite density decreased rapidly from pre-treatment parasite density of 2.87% ± 0.09 to 0.10 % ± 0.01 (3.48% of pre-treatment) at 24 hrs then declined to 0.03 % ± 0.01 (1.22% of pre-treatment) at 48 hours (Figure 1a). The RH+ve parasite fraction remained at this level between Days 2 and 12 after treatment, averaging 0.025% which is 0.87% of the total treated parasite population. This indicates that a very small proportion (<1%) of DHA treated parasites maintained

MMP from Day 2 through Day 12. The RH+ve parasite count started to increase after Day 12, reaching 10% parasitemia at 16.67 ± 0.33 days (n=3 experiments) (Figure 1a).

As expected, the proportions of RH+ve to SG+ve parasites decreased markedly (from 93.79% to 3.33%) 24 hrs after DHA treatment (Figure 2.). This ratio maintained an average of 2.68% between days 1 and 3, and then increased to 52.15% between days 4 and 12. These data indicate that among the very small proportion of parasites stained by SG (~1.5% of pre-treatment) approximately 50% maintained MMP from 4 to 12 days after DHA treatment. The ratio recovered to pre-treatment levels on Day 17, indicating that the majority of parasites have MMP similar to pre-treatment.

Dynamics of RH+ve and SG+ve parasites post atovaquone treatment

Following atovaquone treatment, SG+ve parasite density remained unchanged in the first 24 hrs and declined to ~50% 72 hrs post treatment (Figure 1b). In contrast, RH+ve parasite density decreased rapidly to 0.00 at 72 hrs. Unlike post DHA treatment, no persisting RH+ve stained parasites were detected beyond 72 hours post atovaquone treatment and the culture had not recovered when monitoring ceased at Day 25.

Dynamics of RH+ve and SG+ve parasites after exposure to other artemisinin derivatives

Both ARTA and AS treatments generated similar dynamic patterns to DHA treatment, with a small persisting proportion of RH+ve parasites recovering to 10% in 19 and 21

days, respectively. The density of RH+ve parasites after ARTA and AS treatment was 0.12% ± 0.02 from Day 5 until Day 16 and 0.1% ± 0.01 from Day 2 until Day 15, respectively, when recovery started. (Figure 1c, 1d). The RH+ve parasites constituted 1.3% and 1.04% of the ARTA and AS parasites, respectively.

Micrographs of RH+ve parasites

Figure 3a shows RH+ve parasites, sorted on Day 2 post-DHA treatment, conform with the morphology identified by Teuscher *et al*. [9] and Tucker *et al*. [10], showing blue cytoplasm and condensed red chromatin. In contrast, the RH-ve/SG+ve parasites have collapsed nuclei without cytoplasm. Compared to untreated rings, dormant rings have both compact nuclei (stained by SG) and mitochondrion (stained by RH) consistent with the description by Tucker *et al*. (Figure 3b) [10].

RH+ve parasites are capable of recovery

To demonstrate the viability of parasite populations, FACS sorted RH+ve and RH-ve/SG+ve parasites were serially diluted and cultured until parasitaemia reached 10% or until Day 25 post treatment. Parasite growth was observed in all wells containing RH+ve parasites plated at 10,000 parasites/well, but not in any other cultures (Table 1). 25 days post treatment the 10,000/well culture to reached 10% parasitemia. These results were reproduced in all three experiments.

Transcription of mitochondrial and apicoplast genes in RH sorted parasites

Transcription levels of six genes from major metabolic pathways involving the mitochondria and apicoplast and a control house-keeping gene (*sars*), were determined in both RH+ve and RH-ve/SG+ve parasites. In RH+ve parasites, post-DHA treatment transcription levels of *sars* were reduced to very low levels compared to untreated rings. In contrast, although the transcription levels of the genes involved in the mitochondrial electron transport chain, *coxii*, *sdha* and *uqcr* were all reduced compared to untreated rings they were much higher than *sars*, maintaining above 15% of untreated rings (Figure 4). The apicoplast gene involved in fatty acid synthesis, *bc*, had transcription levels 176.5% of that observed in untreated rings and the gene involved in the lipoic acid metabolism, *lipA*, had transcription levels of 61.85% of untreated rings (Figure 4). No transcription was detected for any of these six genes in the same number of RH-ve/SG+ve parasites. This suggests that the mitochondria/apicoplast complex was active in RH+ve, post-DHA treated parasites, but not active in RH-ve/SG+ve parasites.

Effect of atovaquone on DHA-induced dormant parasites

A number of combination treatments of DHA/ATQ were tested to see if regrowth could be curtailed (Figure 5). When ATQ was added after DHA at IC_{90} level, the time for parasite recovery to 3% parasitemia was 1 day longer than DHA alone. Parasite recovery was further delayed by 6 days when ATQ concentration was at 10x IC_{90} level. There was no parasite recovery at 25 days when the ATQ concentration was 100x IC_{90}.

Discussion

There is growing evidence that parasites enter a state of dormancy after treatment with artemisinin class drugs and a small proportion resume growth, likely causing the clinical recrudescence reported in the field [7]. However, apart from demonstrating parasites recovering following artemisinin treatment [9], direct evidence showing live dormant parasites and their dynamics has not been presented. There is also no reliable method of identifying dormant parasites. Evidence linking dormancy to resistance [11, 14, 31, 32] means that it is critical to easily identify and understand the mechanism parasites use to enter and leave dormancy.

We have recently demonstrated that pyruvate metabolism and fatty acid synthesis pathways in the apicoplast remain active in dormant parasites. This was supported by active transcription of genes encoding key enzymes in these pathways and inhibitors of these pathways delayed recovery of dormant parasites [22]. We have now further demonstrated that mitochondrial activity is present in dormant parasites and is critical for the recovery of dormant parasites. Our data suggest that only parasites with MMP are able to resume growth providing a good biomarker for dormant parasites.

The first approach examined the MMP of parasites following DHA treatment using RH staining. RH is an indicator of MMP and only stains live parasites [27]. We observed that RH stained parasite density declines rapidly from a pre-treatment level of 3.3% to an average of 0.02%. This small population, which is 0.87% of the total treated parasite population, persisted between Day 2 and Day 12 before increasing rapidly with parasite recovery. This indicates only a small subset (<1%) of parasites

retain persisting MMP after exposure to DHA. This proportion is comparable to the recovery rate reported by Teuscher *et al.* [9]. Interestingly, of this persisting population, approximately 50% of parasites retained MMP (RH+ve). In contrast, this persisting RH+ve population was not observed in parasites treated with high doses of atovaquone where no parasite regrowth was observed. ATQ is known to inhibit electron transport in the parasites' mitochondria causing death [21], thus providing a good negative (dead) control. The fact that ATQ treated parasites did not stain with RH at 72 hrs post treatment indicated no persisting dormant parasites following ATQ treatment, evidenced by no recovery of parasites from the culture. This suggests that the RH+ve population were the "seed" for recovery after DHA treatment. A similar pattern was observed in ARTA and AS treated parasites, suggesting this subset of parasites with MMP exist following treatment with artemisinin class drugs.

The second approach was the recovery experiments, where DHA treated parasites were sorted then cultured to see whether they could regrow. This experiment clearly showed that parasites retaining MMP (RH+ve) resumed growth at 10,000/well, while parasites that lost MMP (RH-ve/ SG+ve) failed to recover even at the higher concentration of 5,000,000/well. This demonstrates that only RH+ve parasites are truly dormant parasites, with the ability to regrow. The recovery rate of RH+ve parasites on Day 2 post DHA treatment was estimated to be at a minimum of 1/10,000 (0.01%) because all of the 10,000/well parasite cultures recovered to 10% parasitemia. This rate is lower than that reported earlier [9]. In addition, the time taken for these cultures to reach 10% (25 days) was longer than that required for the unsorted (16 days, Figure 1a) or for dormant parasites (19 days) from earlier experiments [32]. This delay in regrowth could be due to deleterious effect of

staining [33] and the sorting process on the parasites which can take up to 4 hours and during this time the dormant parasites are in PBS at room temperature. Furthermore, the actual sorting through the FACS Aria can cause damage to the sorted cells. There was evidence, on slides made from the sorted parasites, of damage to the parasitised red cells, which would affect viability and reduce rates of recovery.

The third approach was to assess whether a mitochondrial inhibitor could suppress mitochondrial activity in dormant parasites and prevent their recovery. When ATQ was added to DHA treated parasites at lower concentrations, it delayed the parasite recovery by up to 6 days. At 100x IC_{90}, atovaquone stopped the regrowth of dormant parasites. Our previous research showed that treatment with mefloquine after DHA treatment was able to slow the regrowth of dormant parasites. The exact mechanism of mefloquine's action on dormant parasites is not clear.

The fourth approach was measuring transcription levels of several genes associated with the mitochondria and apicoplast in RH+ve and RH-ve parasites. Transcripts of three mitochondrial genes involved in the electron transport and two apicoplast genes were detected in RH+ve parasites. This was not surprising as there is good evidence that together these two organelles provide the metabolic activity required for parasite growth and development during the ring stage [19, 20]. However, this is in sharp contrast to RH-ve/SG+ve parasites where no transcription of these genes was detected. It is likely that mitochondrial activities provide energy to maintain the viability of dormant parasites and power their recovery.

RH-staining also provided an excellent means to determine the morphology of DHA induced dormant parasites. Our data show that RH+ve parasites looked like the "pyknotic" forms described by Teuscher [9] and Tucker [10], not a normal ring stage morphology. In addition, the parasites showed small compact mitochondria as opposed to the branched mitochondrial staining patterns of untreated rings reported by van Dooran *et al.* [34]. In contrast to RH, although SG staining has been used effectively to evaluate parasitemia of *P.falciparum* [35] we found SG cannot distinguish between live and dead parasites as the number of SG+ve parasites decreases much slower after DHA treatment, compared to RH+ve, presumably after DNA decays in dead parasites. These experiments used W2 parasites but the techniques have worked on several parasite strains. Should further studies be undertaken into resistance and dormancy other strains and indeed a variety of strains will need to be used**.**

Combined, these approaches demonstrated that a small subset of parasites maintained MMP and maintained transcription of key enzymes in the mitochondria and apicoplast following exposure to artemisinin class compounds. This subset of parasites was identifiable by RH staining and was responsible for recovery from dormancy. Inhibiting mitochondrial activity following DHA treatment can kill dormant parasites preventing recovery. These findings not only help to understand the dormancy phenomenon that parasites use to escape artemisinin drug pressure, but also provide a means for identifying and purifying dormant parasites following artemisinin treatment. This will greatly enhance our ability to undertake more detailed studies of this parasite stage and may lead to new avenues for better targeting this "Sleeping Beauty" of *P.falciparum* to improve artemisinin efficacy.

Funding

This work was supported by the National Health and Medical Research Council of Australia [grant number: 1021273].

Acknowledgments

We would like to acknowledge the Australian Red Cross for providing human red blood cells and plasma for use in this study. The opinions expressed herein are those of the authors and do not necessarily reflect those of the Australian Defence Force and/or extant Defence Force Policy. No authors of this paper have any conflict of interests.

References:

1. WHO. World Malaria Report. 2012. **World Health Organisation**.

2. White NJ, Nosten F, Looareesuwan S, et al. Averting a malaria disaster. Lancet **1999**; 353:1965-7.

3. Amaratunga C, Sreng S, Suon S, et al. Artemisinin-resistant Plasmodium falciparum in Pursat province, western Cambodia: a parasite clearance rate study. Lancet Infect Dis **2012**; 12:851-8.

4. Kyaw MP, Nyunt MH, Chit K, et al. Reduced susceptibility of Plasmodium falciparum to artesunate in southern Myanmar. PLoS One **2013**; 8:e57689.

5. Noedl H, Se Y, Schaecher K, Smith BL, Socheat D, Fukuda MM. Evidence of artemisinin-resistant malaria in western Cambodia. N Engl J Med **2008**; 359:2619-20.

6. Phyo AP, Nkhoma S, Stepniewska K, et al. Emergence of artemisinin-resistant malaria on the western border of Thailand: a longitudinal study. Lancet **2012**; 379:1960-6.

7. Meshnick SR, Taylor TE, Kamchonwongpaisan S. Artemisinin and the antimalarial endoperoxides: from herbal remedy to targeted chemotherapy. Microbiol Rev **1996**; 60:301-15.

8. Codd A, Teuscher F, Kyle DE, Cheng Q, Gatton ML. Artemisinin-induced parasite dormancy: a plausible mechanism for treatment failure. Malar J **2011**; 10:56.

9. Teuscher F, Gatton ML, Chen N, Peters J, Kyle DE, Cheng Q. Artemisinin-induced dormancy in plasmodium falciparum: duration, recovery rates, and implications in treatment failure. J Infect Dis **2010**; 202:1362-8.

10. Tucker MS, Mutka T, Sparks K, Patel J, Kyle DE. Phenotypic and genotypic analysis of in vitro-selected artemisinin-resistant progeny of Plasmodium falciparum. Antimicrob Agents Chemother **2012**; 56:302-14.

11. Witkowski B, Lelievre J, Barragan MJ, et al. Increased tolerance to artemisinin in Plasmodium falciparum is mediated by a quiescence mechanism. Antimicrob Agents Chemother **2010**; 54:1872-7.

12. LaCrue AN, Scheel M, Kennedy K, Kumar N, Kyle DE. Effects of artesunate on parasite recrudescence and dormancy in the rodent malaria model Plasmodium vinckei. PLoS One **2011**; 6:e26689.

13. Cheng Q, Kyle DE, Gatton ML. Artemisinin resistance in Plasmodium falciparum: A process linked to dormancy? Int J Parasitol Drugs Drug Resist **2012**; 2:249-55.

14. Teuscher F, Chen N, Kyle DE, Gatton ML, Cheng Q. Phenotypic changes in artemisinin-resistant Plasmodium falciparum lines in vitro: evidence for decreased

457 sensitivity to dormancy and growth inhibition. Antimicrob Agents Chemother **2012**;
458 56:428-31.
459 15. Witkowski B, Amaratunga C, Khim N, et al. Novel phenotypic assays for the
460 detection of artemisinin-resistant Plasmodium falciparum malaria in Cambodia: in-
461 vitro and ex-vivo drug-response studies. Lancet Infect Dis **2013**; 13:1043-9.
462 16. Witkowski B, Khim N, Chim P, et al. Reduced artemisinin susceptibility of
463 Plasmodium falciparum ring stages in western Cambodia. Antimicrob Agents
464 Chemother **2013**; 57:914-23.
465 17. Nystrom T, Larsson C, Gustafsson L. Bacterial defense against aging: role of the
466 Escherichia coli ArcA regulator in gene expression, readjusted energy flux and
467 survival during stasis. EMBO J **1996**; 15:3219-28.
468 18. Gray JV, Petsko GA, Johnston GC, Ringe D, Singer RA, Werner-Washburne M.
469 "Sleeping beauty": quiescence in Saccharomyces cerevisiae. Microbiol Mol Biol Rev
470 **2004**; 68:187-206.
471 19. Hopkins J, Fowler R, Krishna S, Wilson I, Mitchell G, Bannister L. The plastid in
472 Plasmodium falciparum asexual blood stages: a three-dimensional ultrastructural
473 analysis. Protist **1999**; 150:283-95.
474 20. Aikawa M. The fine structure of the erythrocytic stages of three avian malarial
475 parasites, Plasmodium fallax, P. lophurae, and P. cathemerium. Am J Trop Med Hyg
476 **1966**; 15:449-71.
477 21. Painter HJ, Morrisey JM, Mather MW, Vaidya AB. Specific role of mitochondrial
478 electron transport in blood-stage Plasmodium falciparum. Nature **2007**; 446:88-91.
479 22. Chen N, LaCrue AN, Teuscher F, et al. Fatty acid synthesis and pyruvate
480 metabolism pathways remain active in dihydroartemisinin-induced dormant ring
481 stages of Plasmodium falciparum. Antimicrob Agents Chemother **2014**; 58:4773-81.

482 23. Vercesi AE, Rodrigues CO, Uyemura SA, Zhong L, Moreno SN. Respiration and
483 oxidative phosphorylation in the apicomplexan parasite Toxoplasma gondii. J Biol
484 Chem **1998**; 273:31040-7.
485 24. Izumo A, Tanabe K, Kato M. A method for monitoring the viability of malaria
486 parasites (Plasmodium yoelii) freed from the host erythrocytes. Trans R Soc Trop
487 Med Hyg **1987**; 81:264-7.
488 25. Kiatfuengfoo R, Suthiphongchai T, Prapunwattana P, Yuthavong Y. Mitochondria
489 as the site of action of tetracycline on Plasmodium falciparum. Mol Biochem Parasitol
490 **1989**; 34:109-15.
491 26. Srinivasan S, Moody AH, Chiodini PL. Comparison of blood-film microscopy,
492 the OptiMAL dipstick, Rhodamine-123 fluorescence staining and PCR, for
493 monitoring antimalarial treatment. Ann Trop Med Parasitol **2000**; 94:227-32.
494 27. Tanabe K. Staining of Plasmodium yoelii-infected mouse erythrocytes with the
495 fluorescent dye rhodamine 123. J Protozool **1983**; 30:707-10.
496 28. Trager W, Jensen JB. Human malaria parasites in continuous culture. 1976. J
497 Parasitol **1976**; 91:484-6.
498 29. Lambros C, Vanderberg JP. Synchronization of Plasmodium falciparum
499 erythrocytic stages in culture. J Parasitol **1979**; 65:418-20.
500 30. Baniecki ML, Wirth DF, Clardy J. High-throughput Plasmodium falciparum
501 growth assay for malaria drug discovery. Antimicrob Agents Chemother **2007**;
502 51:716-23.
503 31. Chavchich M, Gerena L, Peters J, Chen N, Cheng Q, Kyle DE. Role of pfmdr1
504 amplification and expression in induction of resistance to artemisinin derivatives in
505 Plasmodium falciparum. Antimicrob Agents Chemother **2010**; 54:2455-64.

506 32. Chen N, Chavchich M, Peters JM, Kyle DE, Gatton ML, Cheng Q.
507 Deamplification of pfmdr1-containing amplicon on chromosome 5 in Plasmodium
508 falciparum is associated with reduced resistance to artelinic acid in vitro. Antimicrob
509 Agents Chemother **2010**; 54:3395-401.
510 33. Joanny F, Held J, Mordmuller B. In vitro activity of fluorescent dyes against
511 asexual blood stages of Plasmodium falciparum. Antimicrob Agents Chemother **2012**;
512 56:5982-5.
513 34. van Dooren GG, Marti M, Tonkin CJ, Stimmler LM, Cowman AF, McFadden GI.
514 Development of the endoplasmic reticulum, mitochondrion and apicoplast during the
515 asexual life cycle of Plasmodium falciparum. Mol Microbiol **2005**; 57:405-19.
516 35. Izumiyama S, Omura M, Takasaki T, Ohmae H, Asahi H. Plasmodium
517 falciparum: development and validation of a measure of intraerythrocytic growth
518 using SYBR Green I in a flow cytometer. Exp Parasitol **2009**; 121:144-50.
519
520
521

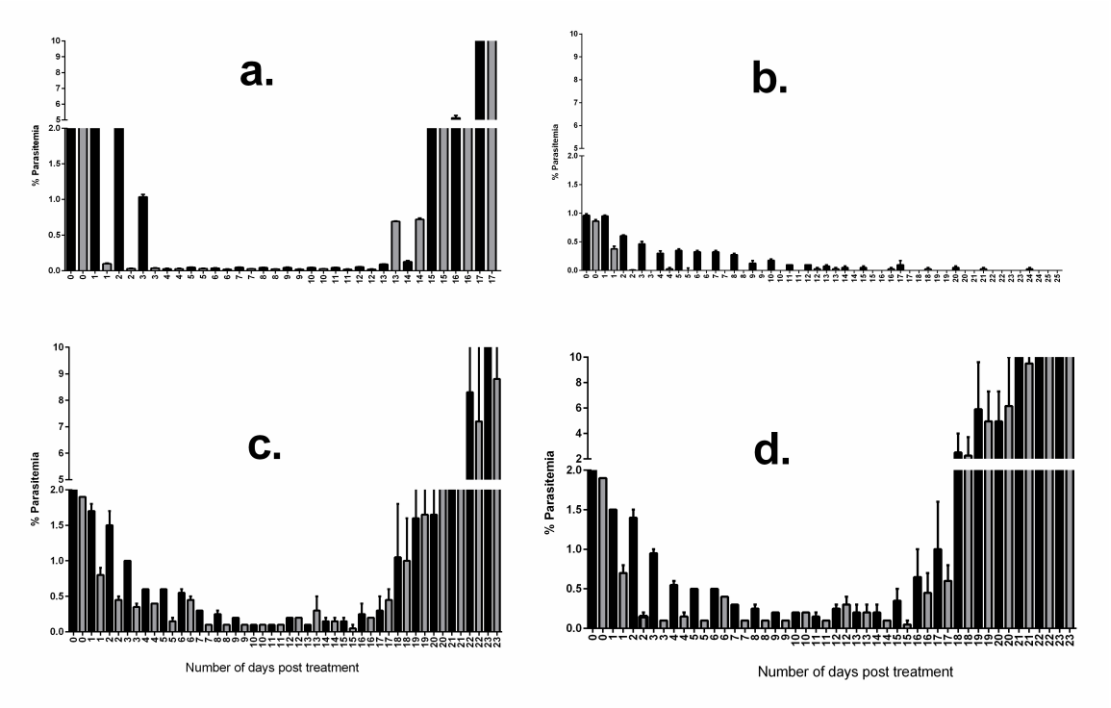

522

523

524 Figure 1. The density of parasites detected by rhodamine 123 (grey) and sybr green
525 (black) staining following dihydroartemisinin (a), atovaquone (b), artelenic acid (c)
526 and artesunate (d) treatment. All cultures started at 2% parasitemia except the
527 atovaquone treated culture which started at 1%. These data are the result of three
528 separate experiments. Mean and SD shown.

529

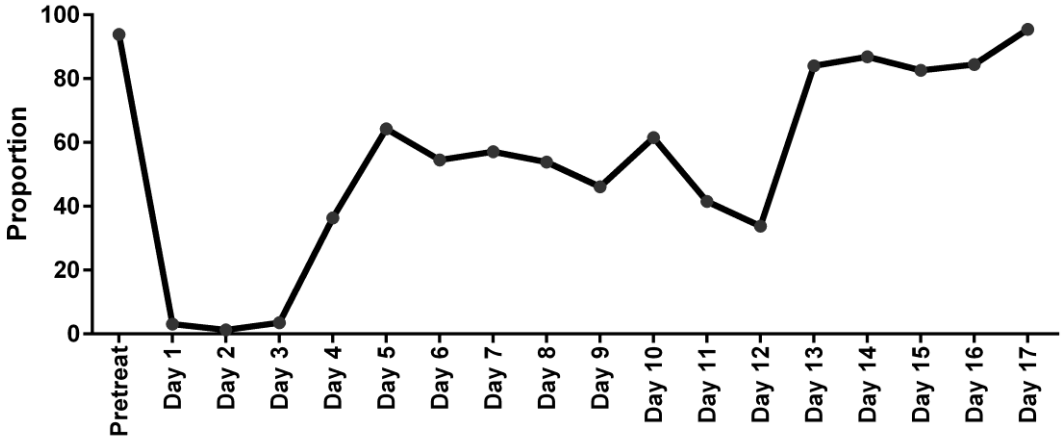

530

531

532 Figure 2. The graph shows the proportion of RH+ve parasites relative to SG+ve

533 parasites after DHA treatment until recovery.

534

535

536

Table 1. Recovery of RH+ve and RH-ve/SG+ve parasites after DHA treatment. Parasites were live sorted by FACS Aria. Cultures with 10, 100, 1000 and 10,000 parasites were then grown to 10% or until day 25 post treatment if no parasites were detected by FACs.

Parasite Population	Parasites per well	Regrowth		
		Well 1	Well 2	Well 3
RH+ve	10	NO	NO	NO
	100	NO	NO	NO
	1000	NO	NO	NO
	10,000	YES	YES	YES
RH-ve /SG+ve	10	NO	NO	NO
	100	NO	NO	NO
	1000	NO	NO	NO
	10,000	NO	NO	NO
	5,000,000	NO	NO	NO

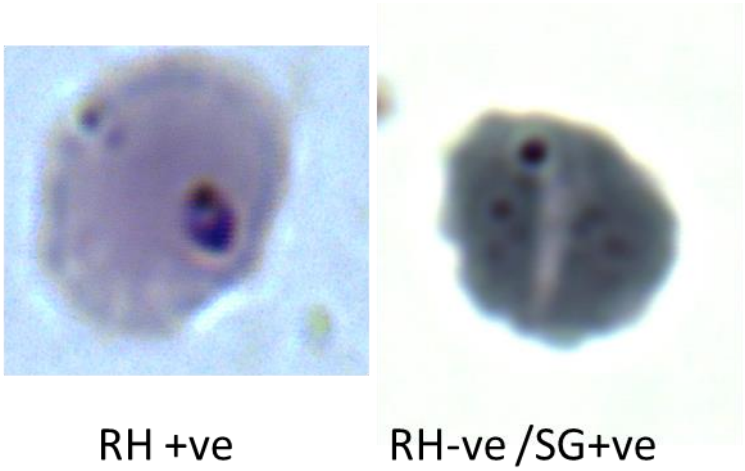

Figure 3a. Micrographs of parasites live sorted by FACS Aria. 100 000 parasites were sorted and then giemsa stained and photographed. The chosen cells are representative of 91 % of all RH+ve cells observed (the rest were uninfected erythrocytes) and 88% for RH –ve/SG+ve cells sorted (the rest were uninfected erythrocytes).

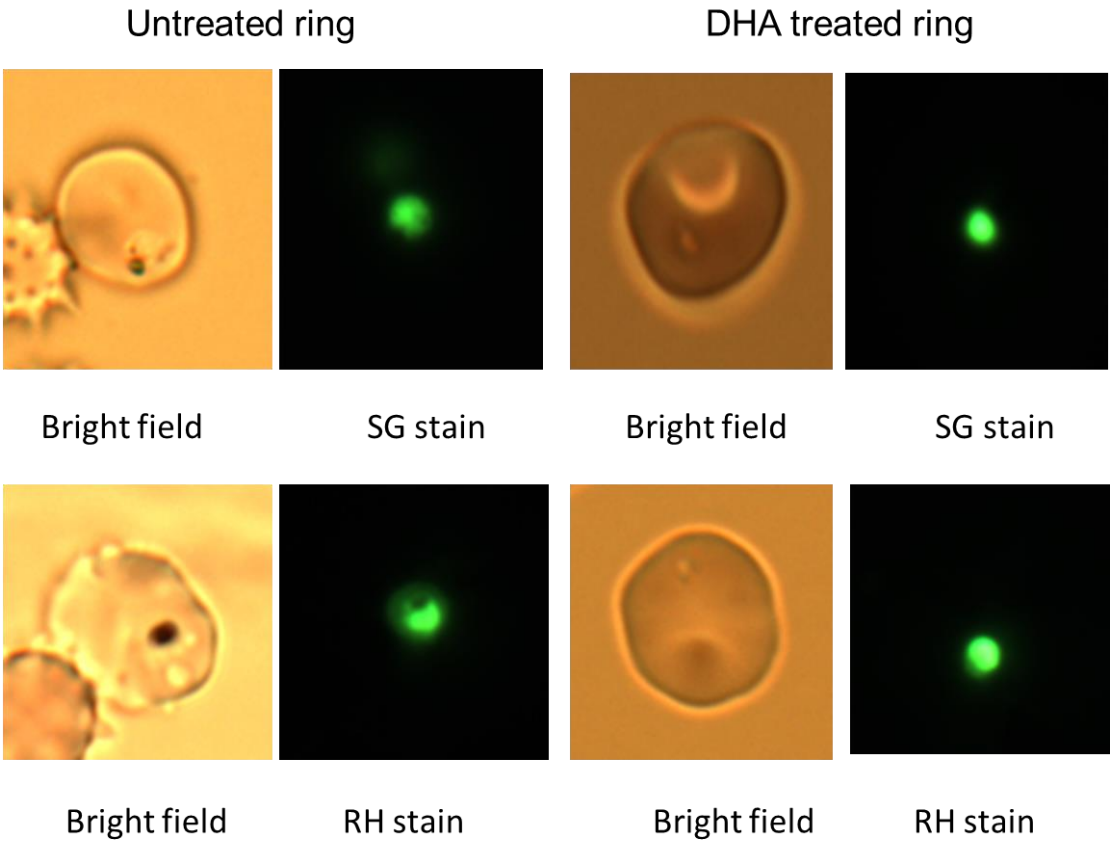

551 Figure 3b. Fluorescent images of *P. falciparum* rings before and after treatment with
552 DHA. Ring stage parasites (after sorbitol treatment) were treated with either and RH
553 or SG and images taken. For DHA treated parasites images were taken on day 2 post
554 treatment.
555

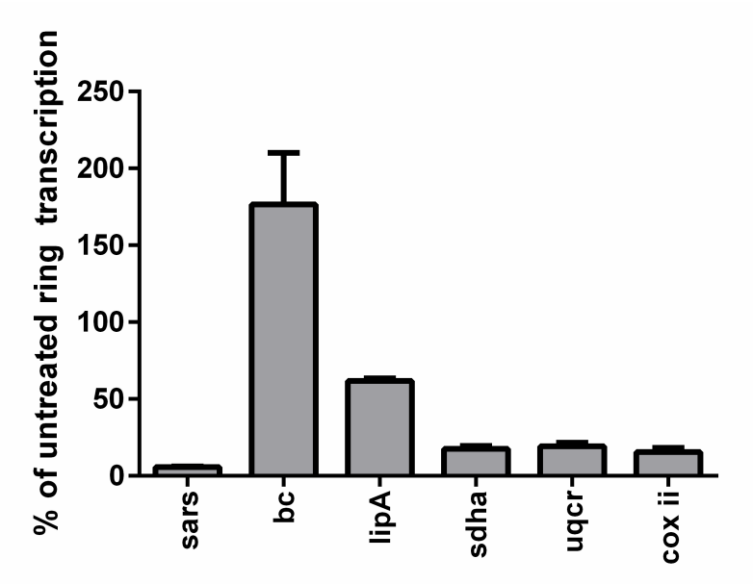

Figure 4. Transcription levels of 6 genes in 20,000 DHA treated, RH+ve parasites relative to 20,000 untreated RH+ve ring stage parasites. The graph shows transcription levels of seryl-tRNA synthetase (*sars*) a control gene and three genes encoding mitochondrial enzymes cytochrome c oxidase subunit II (*coxii*), flavoprotein subunit of succinate dehydrogenase (*sdha*), ubiquinnol-cytochrome c reductase iron-sulfur subunit (*uqcr*) and two genes encoding apicoplast enzymes, lipoyl synthase (*lipA*) and biotin carboxylase subunit of acetyl CoA carboxylase (*bc*) Mean and SD shown.

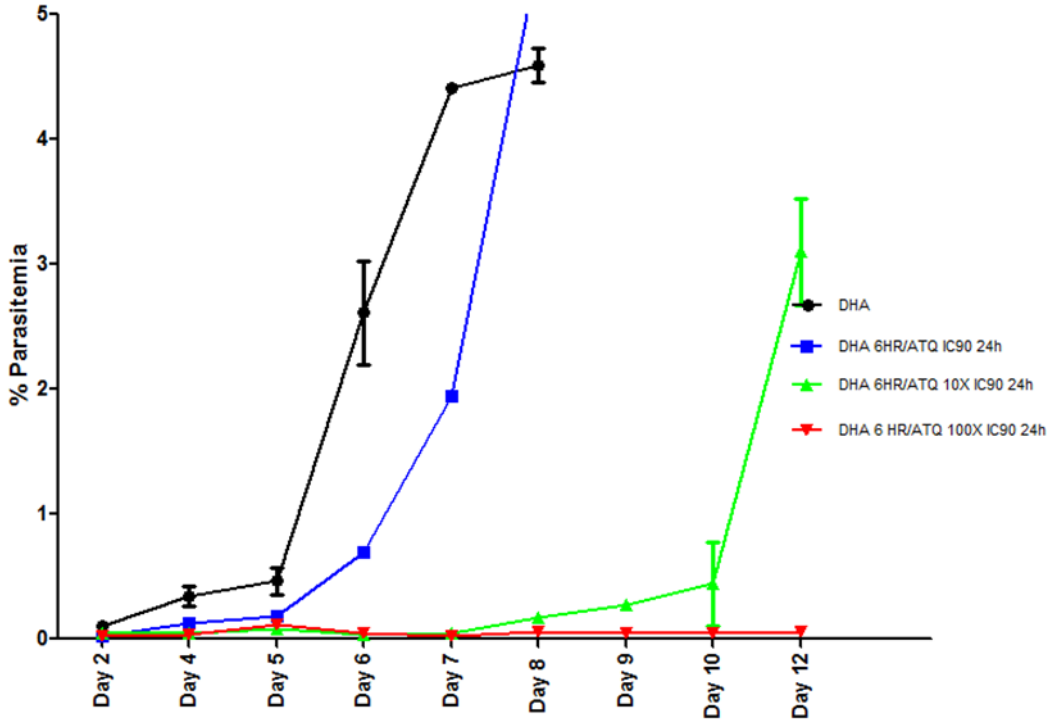

Figure 5. Density of parasites after treatment with DHA and ATQ (IC 90, 10X and 100X)

565

566

567 Figure 5. Density of parasites after treatment with DHA (black line) and ATQ (IC 90

568 [blue], 10X IC90 [green] and 100X IC90 [red]). Mean and SD shown.

569

570

571

572

573